ANNUAL REPORT

31 October 1966

RESEARCH IN SEISMOLOGY

PREPARED FOR

Geophysics Division

Air Force Office of Scientific Research

Arlington, Virginia 22209

By

Department of Geology and Geophysics

Massachusetts Institute of Technology

Cambridge, Massachusetts 02139

Sponsored By

Advanced Research Project Agency

Nuclear Test Detection Office

Project Vela-Uniform

ARPA Order 292-66

Department of Geology and Geophysics
Massachusetts Institute of Technology
Cambridge, Massachusetts 02139

RESEARCH IN SEISMOLOGY

Annual Report

T

Air Force Office of Scientific Research

1 November 1965 - 31 October 1966

ARPA Order No. 292 Amendment 29

Project Code No. 8652

Name of Contractor - M.I.T.

Date of Contract - November 1, 1965

Amount of Contract - $350,198.00

Contract No. AF 49(638)-1632

Contract Termination Date - October 31, 1967

Project Scientists - Frank Press, 617-864-6900, ext 3382
M. Nafi Toksöz, 617-864-6900, ext 6382

Short Title of Work - Research in Seismology

ABSTRACT

The velocity structure in the earth's mantle is determined using the travel times and travel-time slopes of P-waves recorded at LASA. The results show anomalous velocity gradients at depths of 700, 1200, and 1900 km. Both surface wave dispersion data and $dt/d\Delta$ data show the presence of lateral heterogeneities in the upper and lower mantle.

Theoretical studies of acoustic and gravity wave propagation in the atmosphere-ocean systems, effect of aftershocks on free oscillations, and response of layered spherical earth to point sources have been described.

CONTENTS

I.	INTRODUCTION	1
II.	STRUCTURE OF THE EARTH'S MANTLE	2
	A. Body Wave Results	2
	B. Lateral Inhomogeneities in the Upper Mantle from Surface Waves	4
III.	THEORETICAL STUDIES	6
	A. Pulse Propagation in Coupled Systems	6
	B. Effect of Aftershocks on the Measured Period and Q of Free Oscillations	7
	C. Detection of Phases by Least-Squares Filtering	9
	D. Excitation of Free Oscillations and Surface Waves by a Point Source in a Vertically Heterogeneous Earth	12
IV.	SOURCE MECHANISM STUDIES	13
	A. Scaling Law of Seismic Spectrum	13
	B. Earthquake Prediction	15
V.	SEISMIC STATION	17
	FIGURE CAPTIONS	18
	FIGURES	20

I. INTRODUCTION

This is the first Annual Report summarizing our work in "Research in Seismology" under AFOSR contract.

During the year we have initiated the work on a number of problems. A few of these have been completed, but most of them are still in progress. In this report we describe briefly those projects which have been advanced to the stage where, at least, some preliminary results are available.

Our efforts have been directed to several areas. These are: 1) utilization of data from LASA and other sources to study the structure of the earth's interior, 2) theoretical studies of seismic wave propagation and detection methods, 3) source mechanism studies, 4) establishment of a reference seismic station equipped with long period instruments. In the following chapters each one of these areas will be described briefly.

II. STRUCTURE OF THE EARTH'S MANTLE

A. Body wave results.

Seismic body and surface waves generated by earthquakes and underground explosions have been utilized to study the structure of the earth's mantle. Phase and group velocities of the Rayleigh and Love waves in the period range of 80-600 seconds were utilized to interpret the shear wave structure in the upper mantle. The travel times of P-waves from explosions and the travel time slopes ($dT/d\Delta$) measured from LASA recordings were utilized to obtain the compressional velocity profile in the mantle.

Because of its large aperture, geometry, and matched recording system, LASA provides an excellent means of measuring the travel time slopes ($dT/d\Delta$) directly. This in turn can be interpreted in terms of velocity distribution. We have carried out such a study utilizing the $dT/d\Delta$ data computed from LASA recordings of events at distances greater than $\Delta = 30^\circ$, together with the travel times from the Long Shot explosion. To minimize the effect of lateral inhomogeneities in the mantle, the analysis was confined to events arriving from a narrow wedge of azimuth 300-320°, measured clockwise from the north at LASA. Figure 1. defines the band which this wedge covers. Because of the extreme seismicity of the region, a majority

of teleseismic events detected at LASA fall in this range. Furthermore, the Long Shot explosion provides accurate travel time data for the interpretation, and for making static correction to $dT/d\Delta$ curve. This ambiguity arises because of the station corrections at LASA.

The measured $dT/d\Delta$ are compared with the Jeffreys-Bullen model in Figure 2. The discrepencies are well defined and obvious. A new velocity model was computed for the mantle to fit the measured $dT/d\Delta$ and the travel time residuals from the Long Shot. The observed residuals and the curve computed using the new velocity model for the mantle is given in Figure 4. The portion of the model between the surface and the depth of 600 km is based on the surface wave data and other body wave studies. The portion below that, however, satisfy both the travel time residuals and $dT/d\Delta$ measurements. Since the latter is especially sensitive to velocity gradients at depth, the changes in velocity gradients shown at depths of 700, 1200, and 1900 km are reliable and the most interesting features of the lower mantle structure. These and the anomalous region at 350 km depth, constitute a set of "discontinuities" for P-wave velocity profiles in the mantle.

The indications are such that there are lateral variations in the velocity structure of the lower mantle. In Figure 5 $dT/d\Delta$ vs. Δ plots for arrivals to LASA

from two different azimuths are shown. The θ =300-320° azimuth corresponds to the Aleutian-Kurile paths outlined in Figure 1, and the θ =120-140° azimuth to Mexico-Central and South America. The differences in the slopes of $dT/d\Delta$ vs. Δ plots are especially outstanding at regions $\Delta \geq 50^{\circ}$, indicating lateral variations deep in the lower mantle.

B. Lateral Inhomogeneities in the Upper Mantle from Surface Waves.

The lateral inhomogeneities in the uppermost portion of the mantle have been established through seismic refraction studies. At greater depths, complications arise in the use of travel times because of low velocity zone. There are some regional dispersion data and mantle structures. However, most data at periods longer than 100 seconds are computed over mixed paths including continental shields, oceans, and tectonic areas. With certain assumptions, pure path phase velocities have been extracted from composite Love wave data and the corresponding structures computed. These are shown in Figures 6 and 7. The differences in the upper mantle shear velocity profiles are outstanding. Oceanic areas seem to have the lowest velocities in the low velocity zone and the continental shields the highest tectonic regions fall in between.

A technique has been utilized to estimate the temperature differences between oceans and continental shields from the velocity differences shown abcve. With simplifying assumptions this can be written as,

$$\frac{d}{dz}\left[\Delta V(z)\right] = -\frac{d}{dz}\left[\Delta T(z)\right]\left(\frac{\partial V}{\partial T}\right)_p$$

where $\Delta V = V_c - V_0$ is velocity difference, $\Delta T(z)$ temp. difference, $\left(\frac{\partial V}{\partial T}\right)_p$ temperature coefficient of velocity. The last quantity must be determined experimentally. The temperature differences were computed taking various values for $\left(\frac{\partial V}{\partial T}\right)_p$ within the limits of available laboratory data. These are shown in Figure 8. The oceanic upper mantle is characterized by higher temperatures, with the maximum temperature difference being at about 110 km depth.

References

Chinnery, M. A. and M. N. Toksöz, 1966, P-wave velocities in the mantle below 700 km, Bull. Seism. Soc. Am., (in press).

Toksöz, M. N., M. A. Chinnery, and D. L. Anderson, 1966, Inhomogeneities in the earth's mantle, Geophys. Jour., (in press).

III. THEORETICAL STUDIES.

A. Pulse Propagation in Coupled Systems

The theoretical and numerical techniques of pulse propagation in a laterally homogeneous layered atmosphere is extended to coupled systems such as the one formed by the atmosphere and the ocean. The theory was applied to the air-sea waves excited by the explosion of the volcano Krakatoa.

In numerical calculations a standard ARDS atmosphere underlain by a constant-density, constant-velocity ocean was assumed. The atmosphere was terminated by a free surface and the ocean bottom was assumed to be perfectly rigid. The explosive source was placed at the surface of the ocean.

The dispersion curves for the gravity (GR) and acoustic (S) waves in the atmosphere and the classical gravity surface waves in the ocean (GW_o) were computed. These are shown in Figure 9 and 10. The results indicate that free waves in the atmosphere do exist with phase velocities near those of GW_o ($c = \sqrt{gh}$ at long periods). This leads to an efficient transfer of energy from the atmosphere to the ocean and produces sea waves with amplitudes several times larger than hydrostatic. The phase velocity curves for an atmosphere-ocean coupled system are shown in Figure 11. The modifications from that of an atmosphere alone can be seen from the comparison of Figures 9 and 11.

Synthetic barogram and a synthetic marigram were constructed using a surface source with a time function of a single-cycle sine wave of period 40 minutes. These records are shown in Figure 12. The distance corresponds from Krakatoa to San Francisco. The initial pulse is a transient visible both as an atmospheric and oceanic disturbance of sea level with arrival of GW_o mode with hardly any pressure pulse accompanying it.

The scaling laws of atmospheric nuclear explosions applied to the Krakatoa shows that the latter was equivalent to 100-150 megaton explosion.

References

Harkrider, D. G. and F. Press. The Krakatoa air-sea waves: An example of pulse propagation in coupled systems, Geophysical Jour., 1966 (in press).

Press, F. and D. G. Harkrider. The air-sea waves from the explosion of Krakatoa, Science, 1966, (in press).

B. Effect of Aftershocks on the Measured Period and Q of Free Oscillations.

In the estimations of the Q and the eigenfrequencies of the free oscillations of the earth using power spectra, the effects of aftershocks were not taken into account. Since most great earthquakes are followed

by a large number of aftershocks of varying magnitudes, it would be desirable to estimate the effects of these aftershocks on the measured free oscillation spectra.

In formulating the problem of the main event and the aftershocks as a series of K events each of which occurs at time, t_k

$$F_K(t) = \sum_{k=1}^{K} a(t_k)\, f(t - t_k)$$

Let $g(w)\, e^{-i\omega t_k}$ be the spectrum of $f(t - t_k)$ and a_1 be frequency independent amplitude factor for K^{th} event. Now, let's compute the spectral density of the time series, $|\overline{G(\omega)}|^2$, in terms of $|g(\omega)|^2$. Taking the Fourier transform and squaring we obtain,

$$G_K(\omega)\, G_K^*(\omega) = |g(\omega)|^2 \sum_{m=1}^{K} \sum_{k=1}^{K} a(t_k)\, a(t_m)\, e^{-i\omega t_k}\, e^{-i\omega t_m}$$

If it is assumed that both the amplitude and probability of the occurence of events with ~~depth~~ time decreases exponentially as $a(x) = Ae^{-\eta x}$ and $p(x) = \sigma e^{-\sigma x}$, the result reduces to,

$$|\overline{G(\omega)}|^2 = |g(\omega)|^2 A^2 \left\{ \frac{\bar{K}\sigma}{\sigma + 2\eta} + \frac{\bar{K}(\bar{K}-1)\sigma^2}{(\sigma+\eta)^2 + \omega^2} \right.$$

This shows that $|\overline{G(\omega)}|^2$ differs from $|g(\omega)|^2$.

Taking the actual aftershock distribution from Chile Earthquake of 1960, and Alaska Earthquake of 1964, the effects of aftershocks on the Q and eigenfrequency of

main shock were computed. The results of one mode are shown in Figure 13, where a shift in peak frequency of about 0.01 minutes can be seen. The Q is increased from 205 to 250.

On the basis of calculations it is concluded that the aftershock sequences can affect the position and shape of spectral peaks by a finite amount. The magnitude of the change of the peak frequency is, in general, too small to affect the interpretation. The errors introduced in Q measurements are greater and become significant at shorter periods.

References

Press, F., Spectra of free oscillations from an aftershock sequence, Geophys. J., 1966, (in press).

Press, F., Free Oscillations, Aftershocks and Q, in "The Earth Beneath the Continents", AGU Monograph No. 10, 1966 (in press).

C. Detection of Phases by Least Squares Filtering.

The initial P-motion is probably the most easily detectable phase on a seismogram. The signal and the microseismic noise, in general, posess different statistical properties and various techniques can be used

to enhance the signal-to-noise ratio. The later P-phases (such as pP, PP, PcP) are in general less suitable for purely statistical treatment. However, these later events may be expressed as filtered versions of the initial P-wave.

Here we describe a scheme of detecting these late P-phases given the initial P-wave motion. The technique involves finding short filters which match the P-wave to later phases of the seismograms by minimizing the squared error. The mean square error determines the quality of the fit and can be used as the detection criterion.

The simplest formulation for the noise free case can be given as follows:

Let

$\bar{x} = \text{Col}(x_0, x_1, \ldots x_n)$ be the input signal (i. e. initial P-wave),

$\bar{f} = \text{Col}(f_0, f_1, \ldots f_k)$ be the filter to be determined and,

$\bar{d} = \text{Col}(d_0, d_1, \ldots d_{n+k+1})$

be the desired output. This could be any portion of the seismogram where we wish to test if it matches the initial P-wave. Let us define a matrix

$$\bar{X} = \begin{bmatrix} x_0 & 0 & \cdots & 0 \\ x_1 & x_0 & & \vdots \\ \vdots & \vdots & & \\ x_n & \vdots & & x_0 \\ 0 & x_n & & x_1 \\ \vdots & \vdots & & \vdots \\ 0 & 0 & & x_n \end{bmatrix}$$

Let us find $\bar{f}$ such that the error

$$\bar{e} = \bar{X}\bar{f} - \bar{d}$$

has minimum power. The minimization criteria enable us to find $\bar{f}$. The mismatch between $\bar{X}$ and $\bar{d}$ can be measured in terms of normalized mean square error $\mathcal{E}$.

$$\mathcal{E} = 1 - \frac{\bar{f}^T(X^T\bar{d})}{\bar{d}^T\bar{d}}$$

For perfect match $\mathcal{E}=0$ and for no match $\mathcal{E}=1$.

In practical application we take the initial P-wave, specify the length of $\bar{f}$, and slide it along the seismogram at each point computing f_i and $\mathcal{E}$. Where there is a matching P-phase, $\mathcal{E}$ becomes small.

An example of this scheme is shown as applied to LASA recordings (Figure 14) of the Long Shot event. In Figure 15. we show the "performance parameter"

$$F = \bar{f}^T(X^T\bar{d})$$

The maxima of F correspond to arrival of phases. The crustal reverberations and the PcP are clearly visible in the Figure 14, while the original seismogram does not show the reverberations as clearly.

Reference

Toksöz, M. N., C. W. Frasier, and S. Treitel, "Detection of seismic arrivals by least-squares match filtering", Presented at the 36th Annual International Meeting of the Society of Exploration Geophysicists. Nov. 6-10, 1966, Houston, Texas.

D. Excitation of Free Oscillations and Surface Waves by a Point Source in a Vertically Heterogeneous Earth.

Radiation patterns of surface waves and free oscillations for vertically heterogeneous elastic media are derived for arbitrary sources using variational equations. The results are expressed in terms of normal mode solutions and source functions, and show that for a spherical earth the radiation patterns can be constructed from normal mode solutions alone. Source functions for a single force, a single couple, and double ccuple without torque, all in arbitrary directions, are derived.

Reference

Saito, M., "Excitation of Free Oscillations and Surface Waves by a Point Source in a Vertically Heterogeneous Earth.". J. Geophys. Res., 1966, (in press).

IV. SOURCE MECHANISM STUDIES

A. Scaling Law of Seismic Spectrum

The dependence of the amplitude spectrum of seismic waves on source size is investigated on the basis of two dislocation models of an earthquake source. One of the models is due to Haskell and is called the ω^3 model. The other is called the ω^2 model, and is constructed by fitting an exponentially decaying function to the autocorrelation function of the dislocation velocity. The number of source parameters is reduced to one by the assumption of similarity. We found that the most convenient parameter for our purpose is the magnitude, M_s, defined for surface waves with period of 20 seconds. Spectral density curves are determined for given M_s.

Comparison of the theoretical curves with observations is made in two different ways. The observed ratio of the spectra of seismic waves with the same propagation path but from earthquakes of different sizes are compared with the corresponding theoretical ratio, thereby eliminating the effect of propagation on the spectrum. The other method is to check the theory with the empirical relation between different magnitude scales defined for different waves at different periods. The ω^2 model gives a satisfactory agreement with such observations on the assumption of similarity, but the ω^3 model does not.

(See Figure 16.)

The assumption of similarity implies a constant stress drop independent of source size. The stress drop in earthquakes may be estimated from the spectral density of surface waves at long periods, if the fault length and offset are known from field measurements. A preliminary study of Love waves from the Parkfield earthequake of June 28, 1966, shows that the stress drop at the source of this earthquake is lower than the normal value (around 100 bars) by about two orders of magnitude. This result implies that a single parameter, such as magnitude, cannot describe an earthquake even as a rough measure.

Reference

Aki, K., Scaling Law of Seismic Spectrum, J. Geophys. Res., 1966, (in press).

B. Earthquake Prediction

Recent evidence from the field and laboratory investigations are reviewed to make a critical evaluation of the feasibility of earthquake prediction. Possible mechanisms of the shallow earthquakes are stated and the effects of pore pressure, water weaking, lubrication, and creep fracture are discussed.

There are some field and laboratory data on the premonitory indications of an earthquake. Forewarning may come from three sources:

1. Observed deformation before an earthquake such as tilts and strain in epicentral region (These have been observed and documented in Japan).

2. The general increase in the number of small events prior to the main shock (or failure) have been observed in the laboratory.

3. Changes in physical properties of rocks near the fault may take place as they are strained. In the laboratory a drop in seismic velocities has been detected as the rock stressed to the point of failure. Also, a significant decrease in the electrical resistivity has been measured as the stress is increased to the critical value.

Suggestions have been made for the instrumentation

of seismic belts along major faults. Type of instruments, and field clusters and general field investigations have been evaluated.

Reference

Press, F. and W. F. Brace, Earthquake Prediction, Science, 152, 1575-1584, June 17, 1966.

V. SEISMIC STATION

A seismic station to be equipped with long period instruments is being completed at Harvard, Massachusetts. This will be a reference station for long period recordings, and testing and calibration of the similar field instruments. The seismic vault is being made available by the Harvard University. At the present some repairs and modifications of the vault are being completed.

Initially the station will contain a two-component Benioff tiltmeter (Mercury pendulum), two-component quartz rod strain meters, and a long period vertical seismometer with displacement transducer. In addition to these some experimental tilt and strain devices will be placed at the vault for testing.

The construction of the tiltmeters and all analog recording systems have been completed. Currently a number of digital recording devices are being evaluated. It is anticipated that analog data from tiltmeters will be available in six weeks, and those from strainmeters in less than three months.

FIGURE CAPTIONS

Fig. 1 Locations of the LASA and the Long Shot nuclear explosion. The dashed lines outline the aximuth range 300°-320° from LASA.

Fig. 2 Observed dt/dΔ for all events in the azimuth range 300°-320° detected at LASA. The dashed curve is the adopted "mean" curve.

Fig 3 The comparison of the observed dt/dΔ ("good" events from Figure 7) and the theoretical values from Model 77.

Fig. 4 Compressional velocity profile of the Mantle Model 77, with the Jeffreys-Bullen model for comparison. Boxes show the regions of the "discontinuities".

Fig. 5 Observed dt/dΔ for all events from the azimuth ranges 300-320° and 140-160° from the LASA. These deomonstrate the differences between the two different paths.

Fig. 6 Observed composite path Love wave data and the extracted "pure-path" phase velocities.

Fig. 7 Upper mantle shear velocity models for the oceanic, continental shield, and tectonic regions. Below 500 km profiles are uncertain because of insufficient data.

Fig. 8 Temperature differences under oceans and continents with dV/dT as a parameter. A constant value (C) can be added to or subtracted from each temperature profile.

Fig. 9 Phase and group velocity dispersion curves for several modes of ARDC standard atmosphere with free surface at 220 km.

Fig. 10 Phase and group velocity dispersion curves for fundamental gravity wave in a constant-velocity, constant-density ocean of 5 km thickness.

Fig. 11 Phase velocity dispersion curves for modes of the air-ocean system.

Fig. 12 Synthetic barogram (upper) and marigram (lower) for San Francisco. Source time function is a single-cycle sine wave of 40 minute period. Time is local civil time, August 27, 1883.

Fig. 13 Spectra of main shock (crosses) and main plus aftershock sequence (circles) for Chilean earthquake of 1960. For this case, Q assumed at 200, T_0 = 10.0 minutes. Peak frequency shift is .01 minutes, Q shifts to 250.

Fig. 14 Long Shot seismograms of A_0 and B ring of LASA. Each trace is a composite (sum) of 25 seismometer outputs.

Fig. 15 "Performance factor" for traces shown in Fig. 14.

Fig. 16 Theoretical relation between M_B and M_S based on the W-square model, as compared with that observed by Gutenberg and Richter.

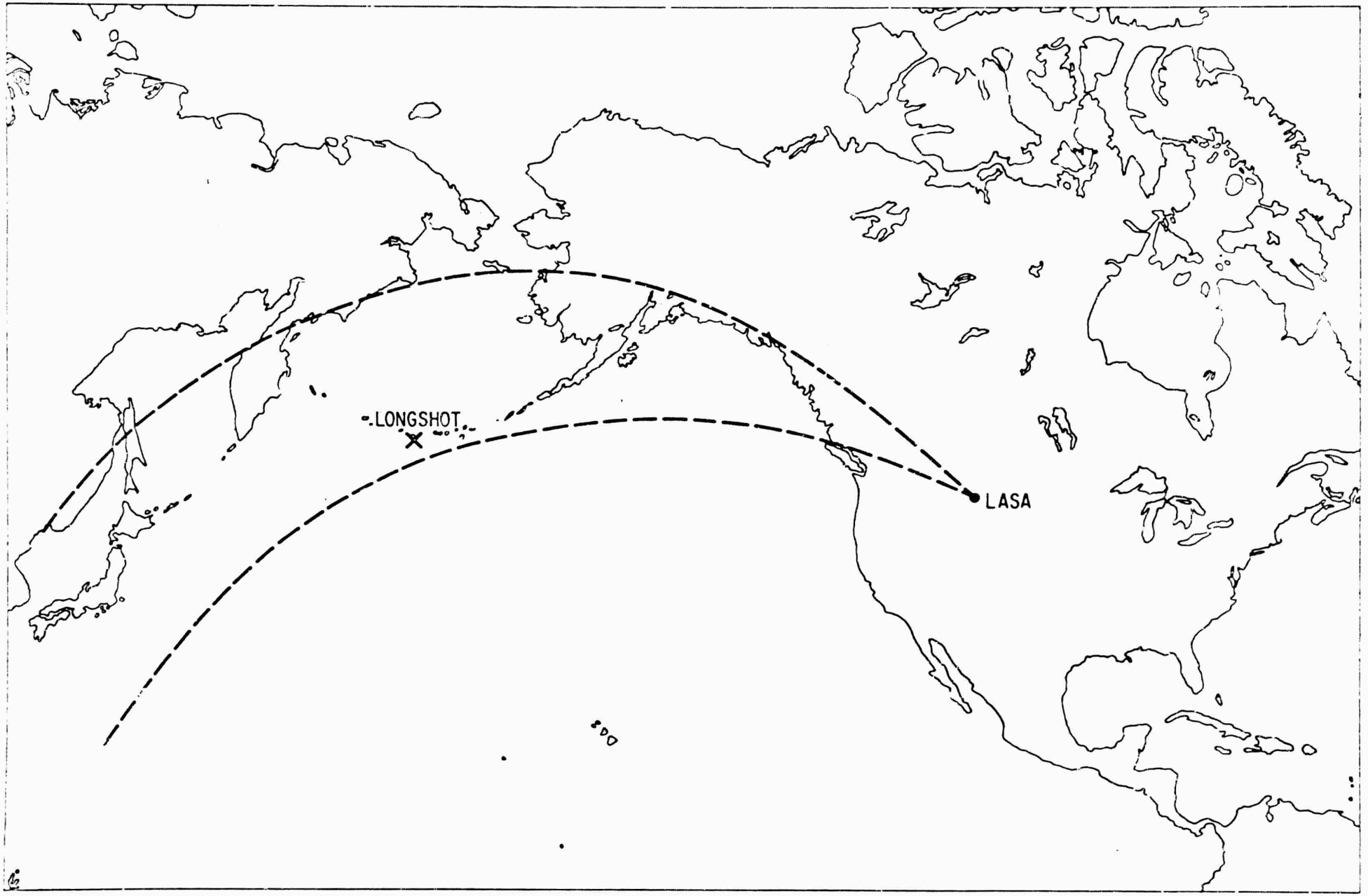

Fig. 1

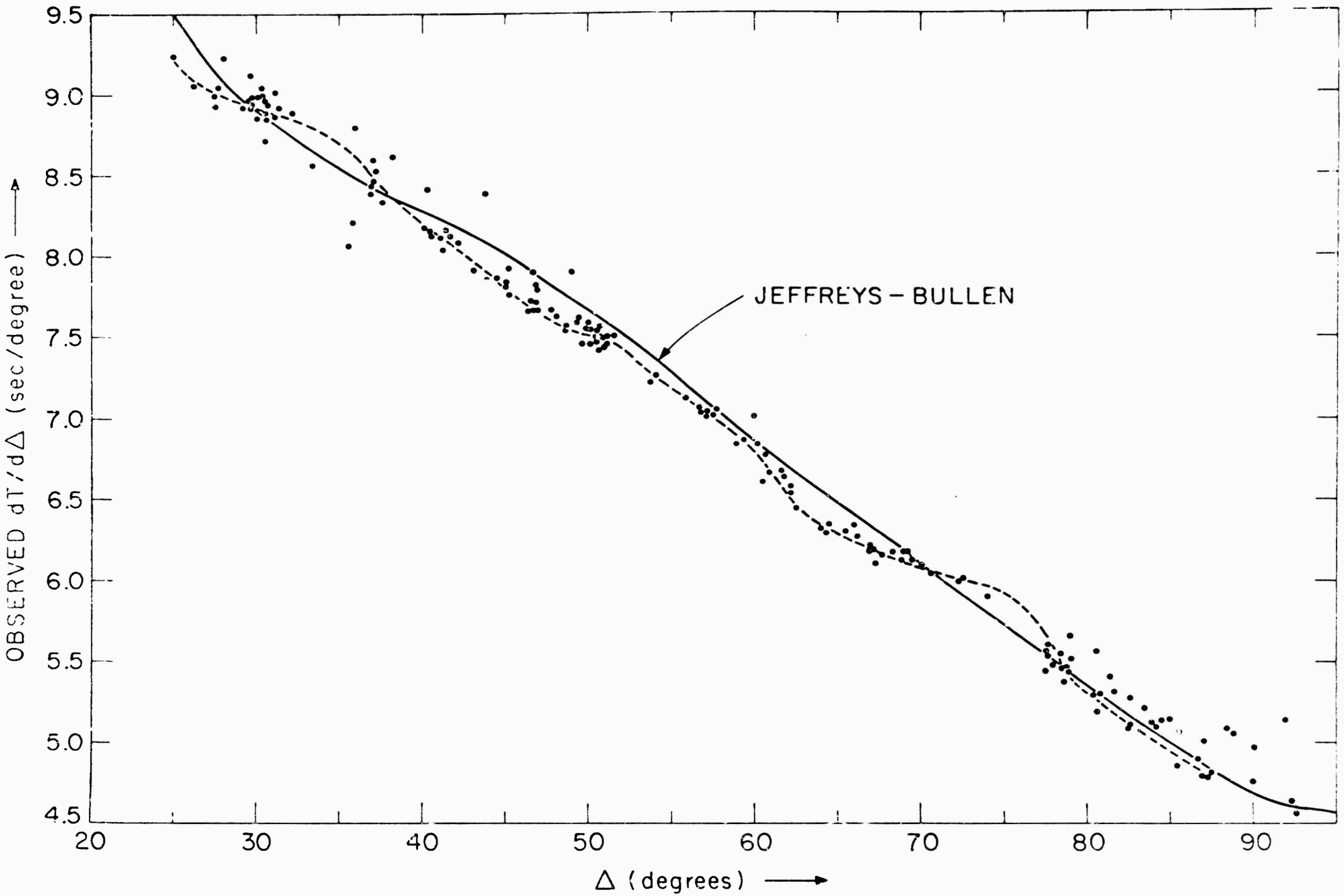
9.5
9.0
8.5
8.0
7.5
7.0
6.5
6.0
5.5
5.0
4.5
OBSERVED dT/dΔ (sec/degree)
20
30
40
50
60
70
80
90
Δ (degrees)
JEFFREYS – BULLEN

Fig. 2

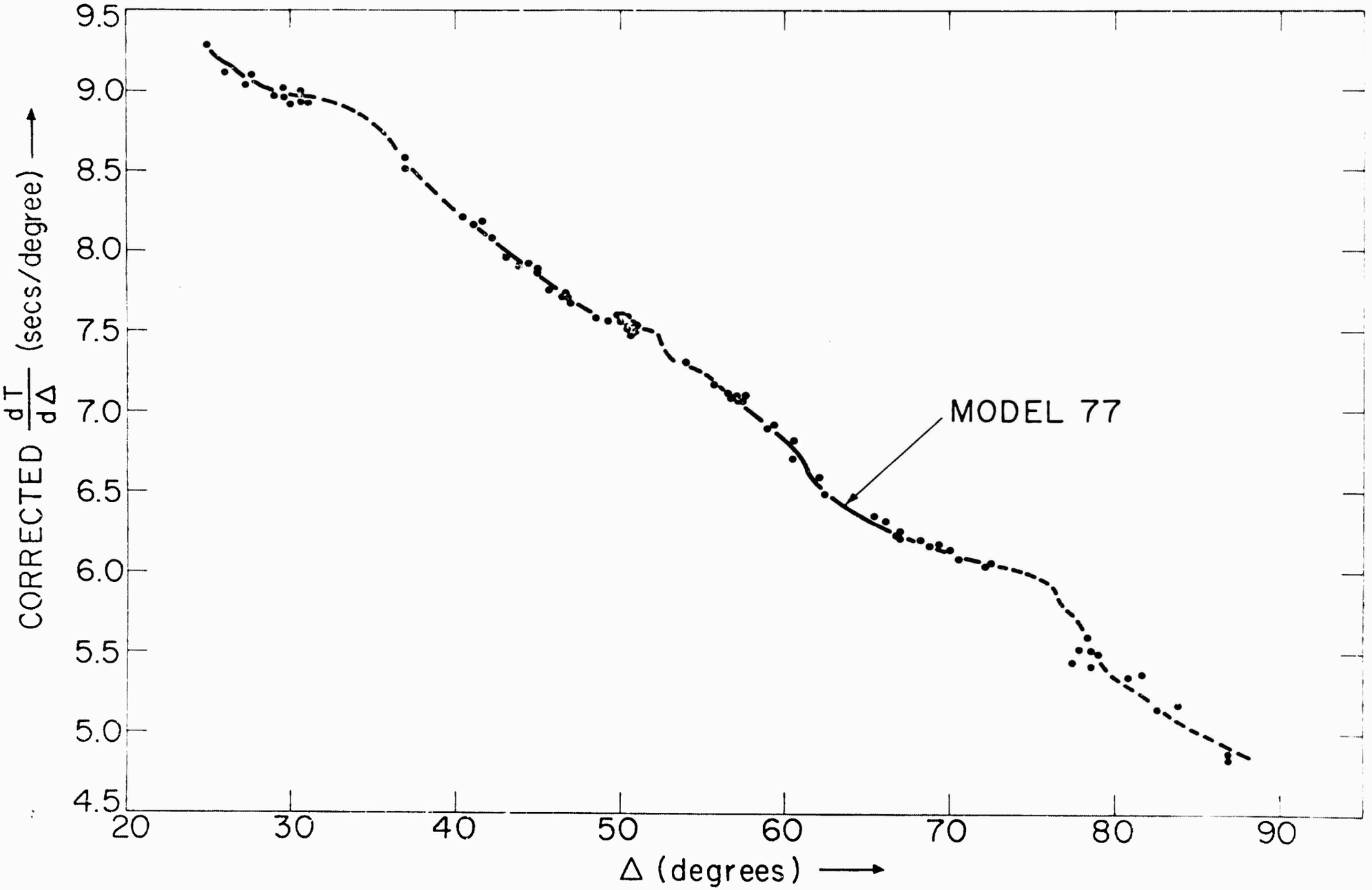
9.5
9.0
8.5
8.0
7.5
7.0
6.5
6.0
5.5
5.0
4.5
CORRECTED $\frac{dT}{d\Delta}$ (secs/degree) ⟶
MODEL 77
20
30
40
50
60
70
80
90
Δ (degrees) ⟶

Fig. 3

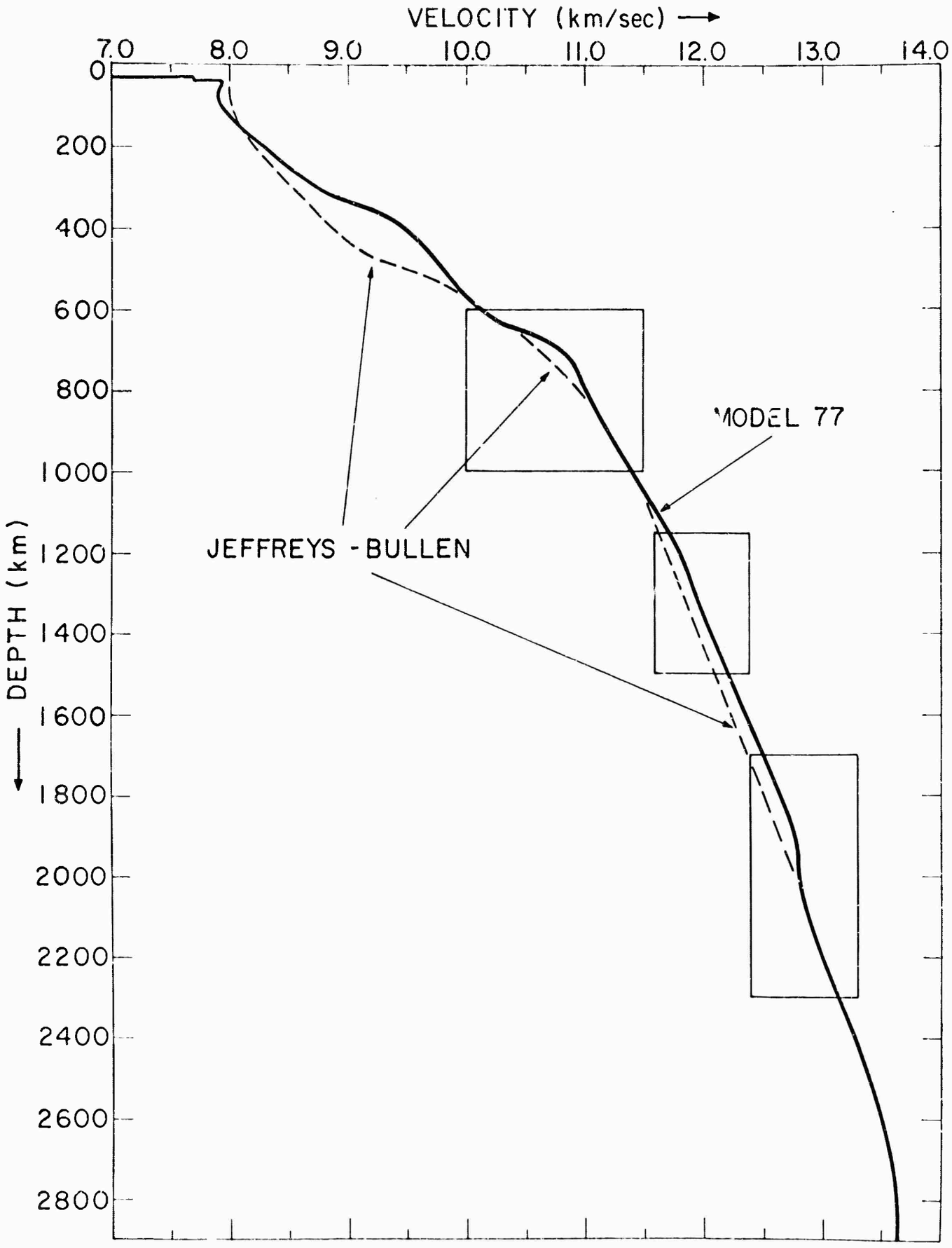
VELOCITY (km/sec) →
7.0
8.0
9.0
10.0
11.0
12.0
13.0
14.0
0
200
400
600
800
1000
1200
1400
1600
1800
2000
2200
2400
2600
2800
DEPTH (km)
MODEL 77
JEFFREYS - BULLEN

Fig. 4

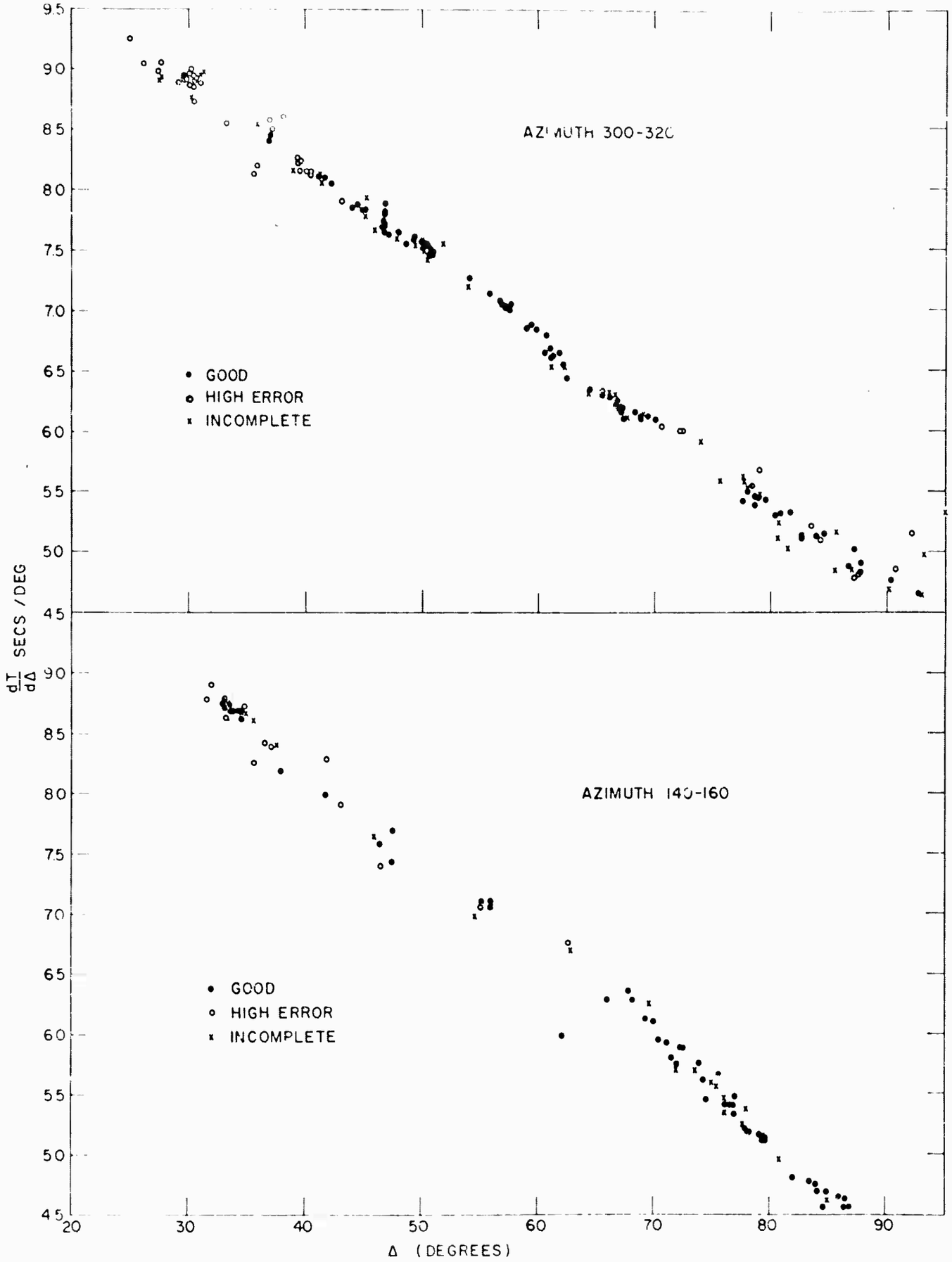
AZIMUTH 300-320
GOOD
HIGH ERROR
INCOMPLETE
AZIMUTH 140-160
GOOD
HIGH ERROR
INCOMPLETE
dT/dΔ SECS/DEG
Δ (DEGREES)
9.5
9.0
8.5
8.0
7.5
7.0
6.5
6.0
5.5
5.0
4.5
20
30
40
50
60
70
80
90

Fig. 5

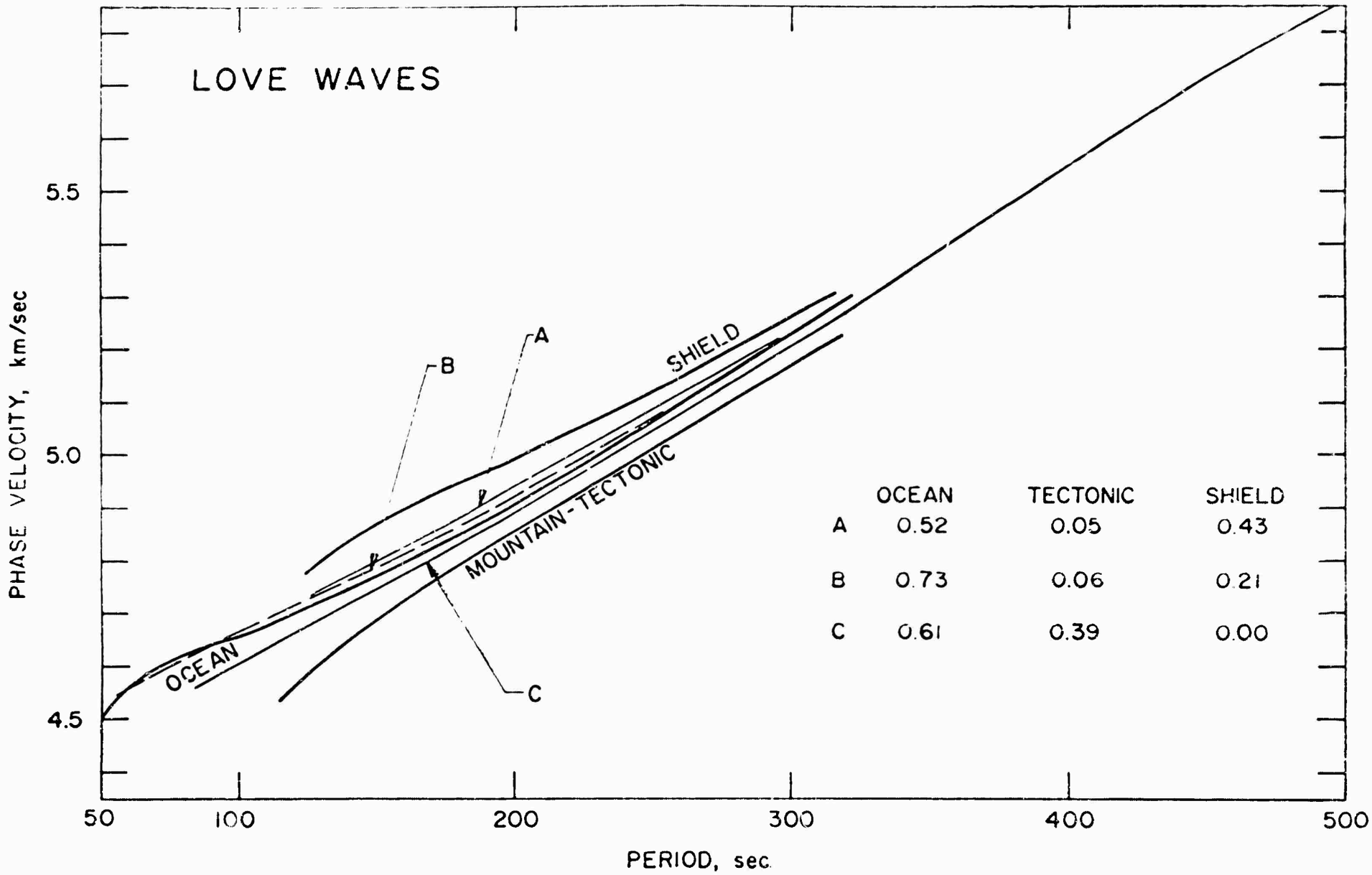
LOVE WAVES
PHASE VELOCITY, km/sec
5.5
5.0
4.5
50
100
200
300
400
500
PERIOD, sec.
A
B
C
SHIELD
MOUNTAIN-TECTONIC
OCEAN
OCEAN TECTONIC SHIELD
A 0.52 0.05 0.43
B 0.73 0.06 0.21
C 0.61 0.39 0.00

Fig. 6


SHEAR VELOCITY (km / sec)
100
200
300
400
500
600
700
800
900
1000
1100
SHIELD
OCEANIC
TECTONIC
?
3.0
3.0
4.0
4.5
5.0
5.5
6.0
6.5

Fig. 7

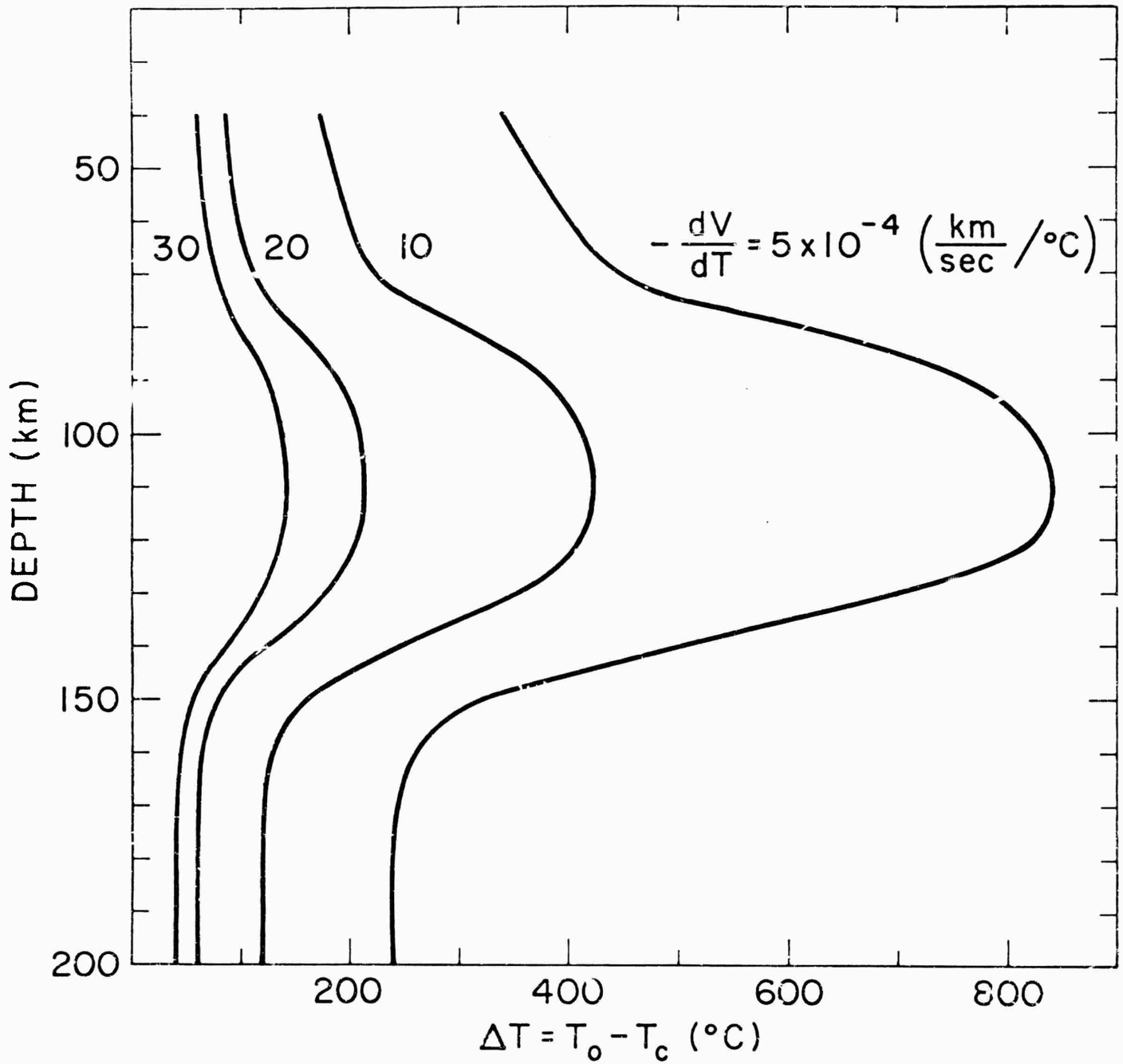
50
100
150
200
DEPTH (km)
30
20
10
$-\frac{dV}{dT} = 5 \times 10^{-4} \left(\frac{km}{sec}/°C\right)$
200
400
600
800
$\Delta T = T_o - T_c$ (°C)

Fig. 8

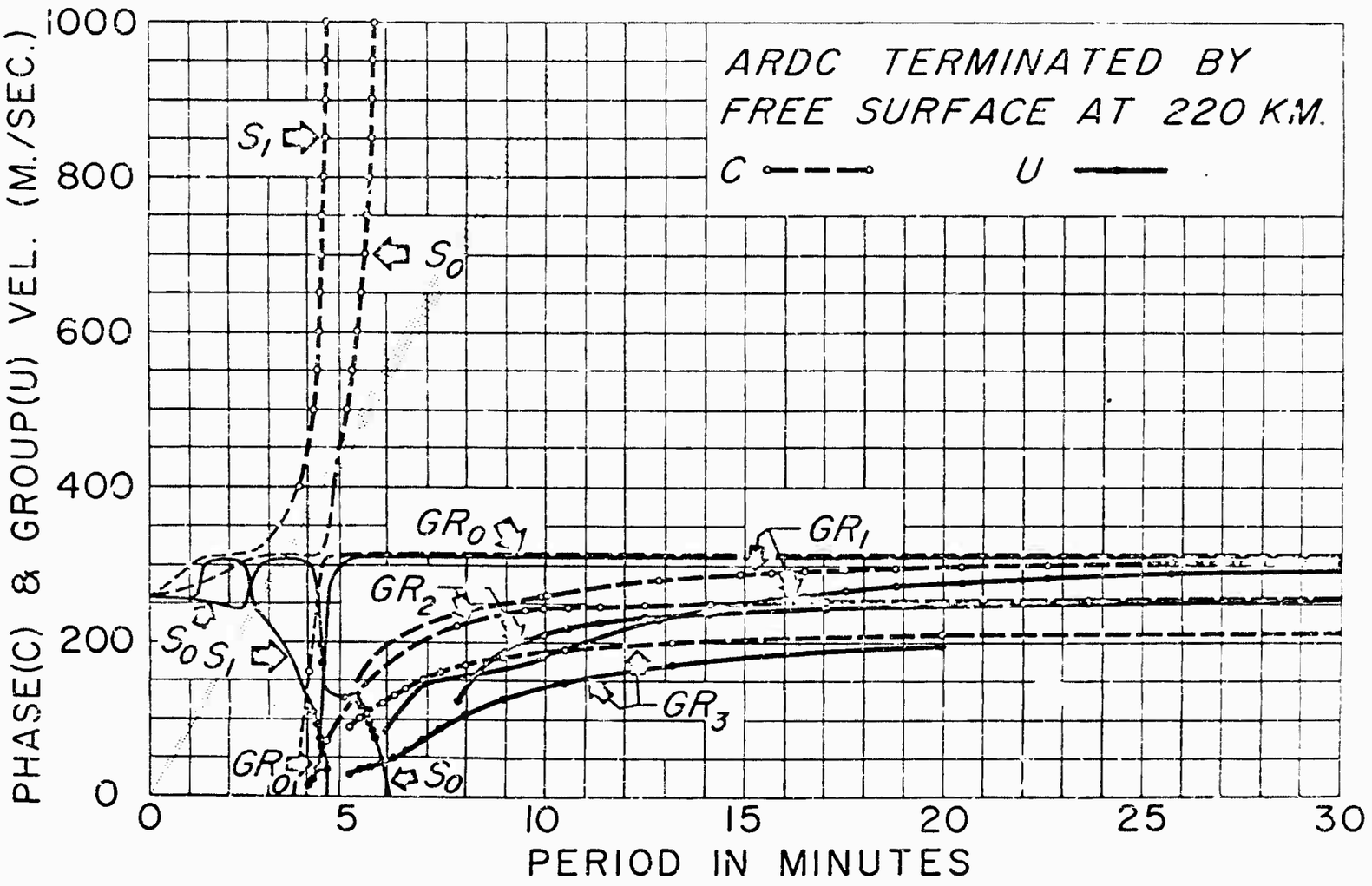
ARDC TERMINATED BY
FREE SURFACE AT 220 K.M.
C
U
PHASE(C) & GROUP(U) VEL. (M./SEC.)
1000
800
600
400
200
0
0
5
10
15
20
25
30
PERIOD IN MINUTES
S_1
S_0
GR_0
GR_1
GR_2
GR_3
S_0 S_1
GR_{01}
S_0

Fig. 9

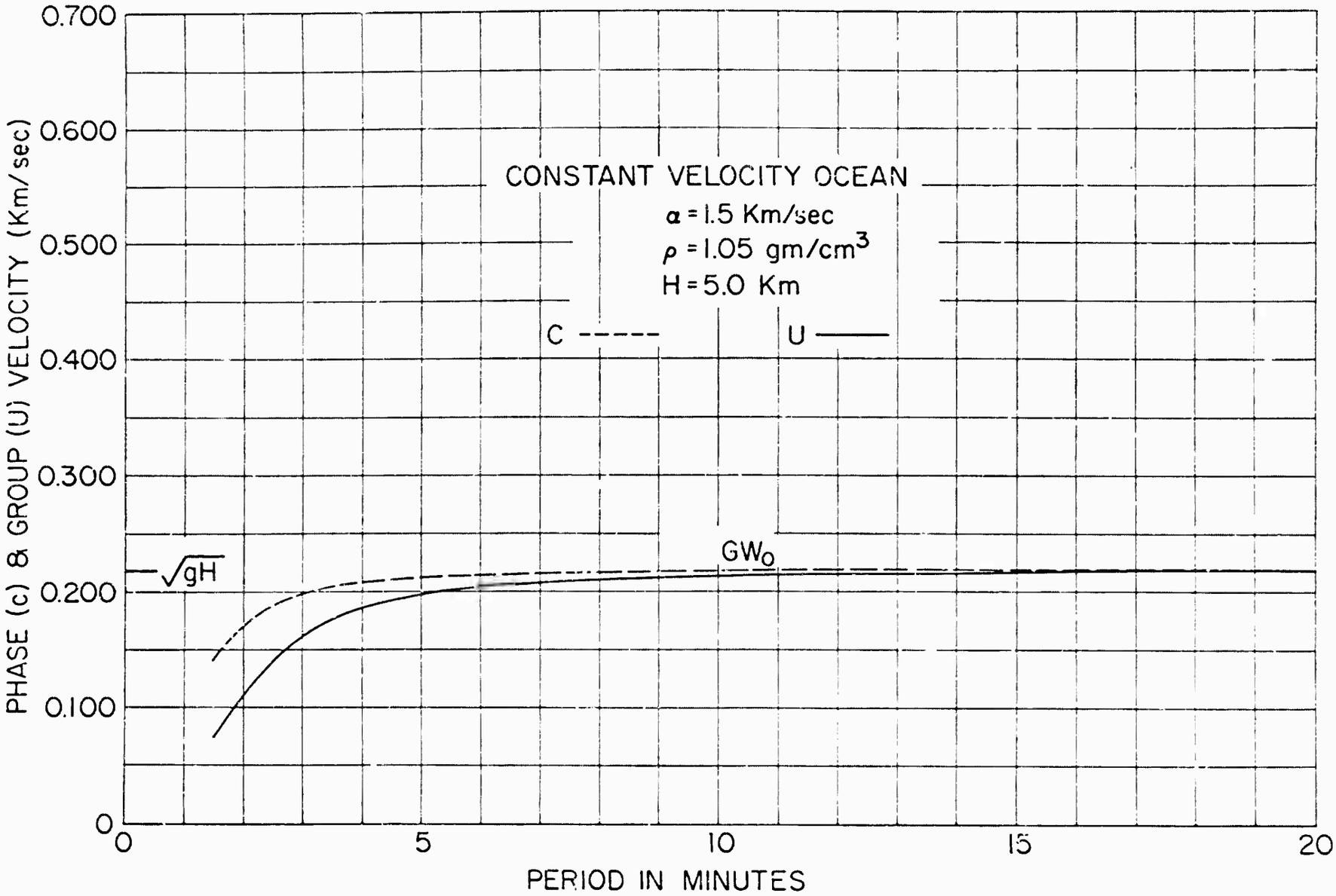
CONSTANT VELOCITY OCEAN
α = 1.5 Km/sec
ρ = 1.05 gm/cm³
H = 5.0 Km
C
U
GW₀
√gH
PHASE (c) & GROUP (U) VELOCITY (Km/sec)
PERIOD IN MINUTES
0.700
0.600
0.500
0.400
0.300
0.200
0.100
0
0
5
10
15
20

Fig. 13

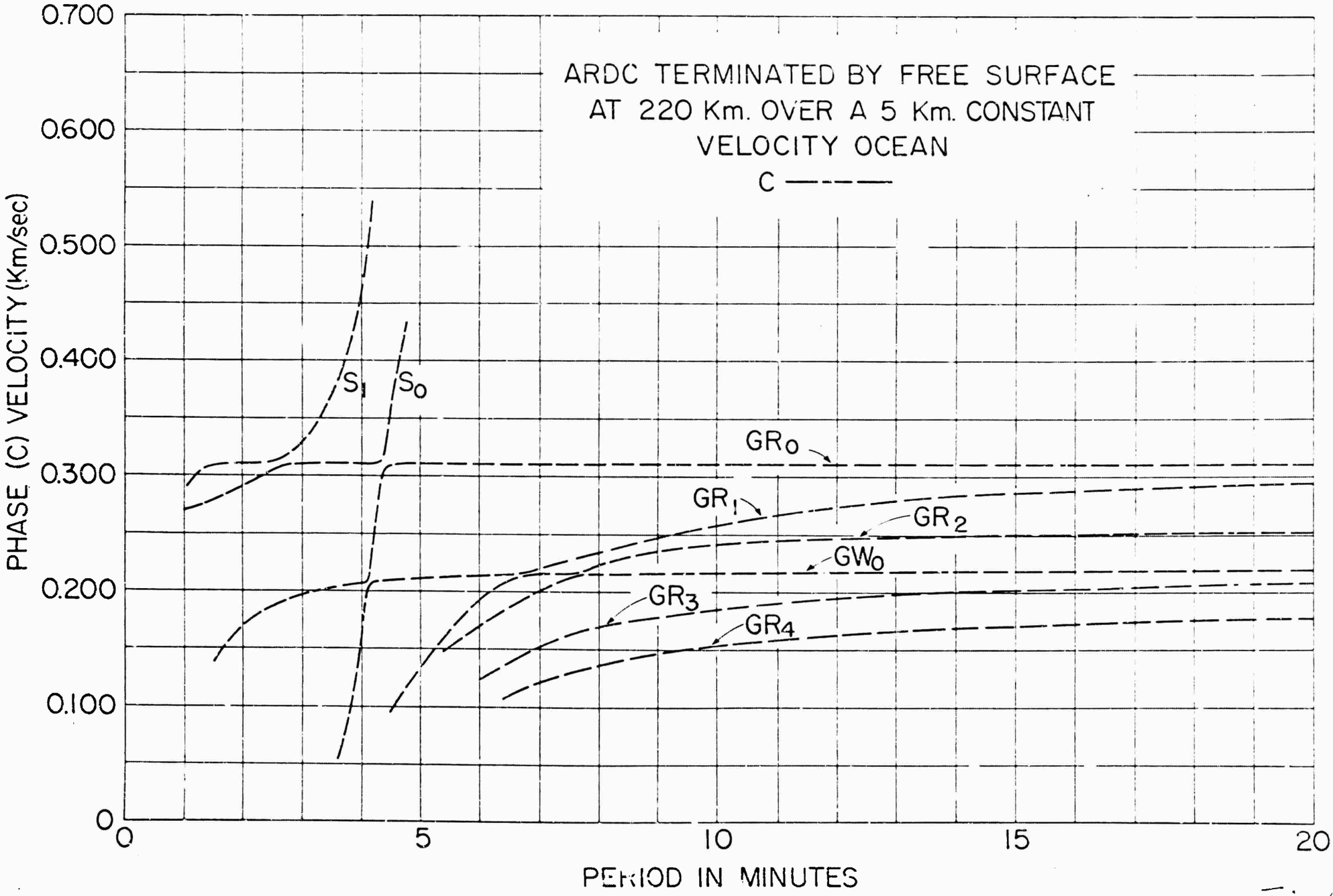
ARDC TERMINATED BY FREE SURFACE
AT 220 Km. OVER A 5 Km. CONSTANT
VELOCITY OCEAN
C
PHASE (C) VELOCITY (Km/sec)
0.700
0.600
0.500
0.400
0.300
0.200
0.100
0
0
5
10
15
20
PERIOD IN MINUTES
S1
S0
GR0
GR1
GR2
GW0
GR3
GR4

Fig. 11

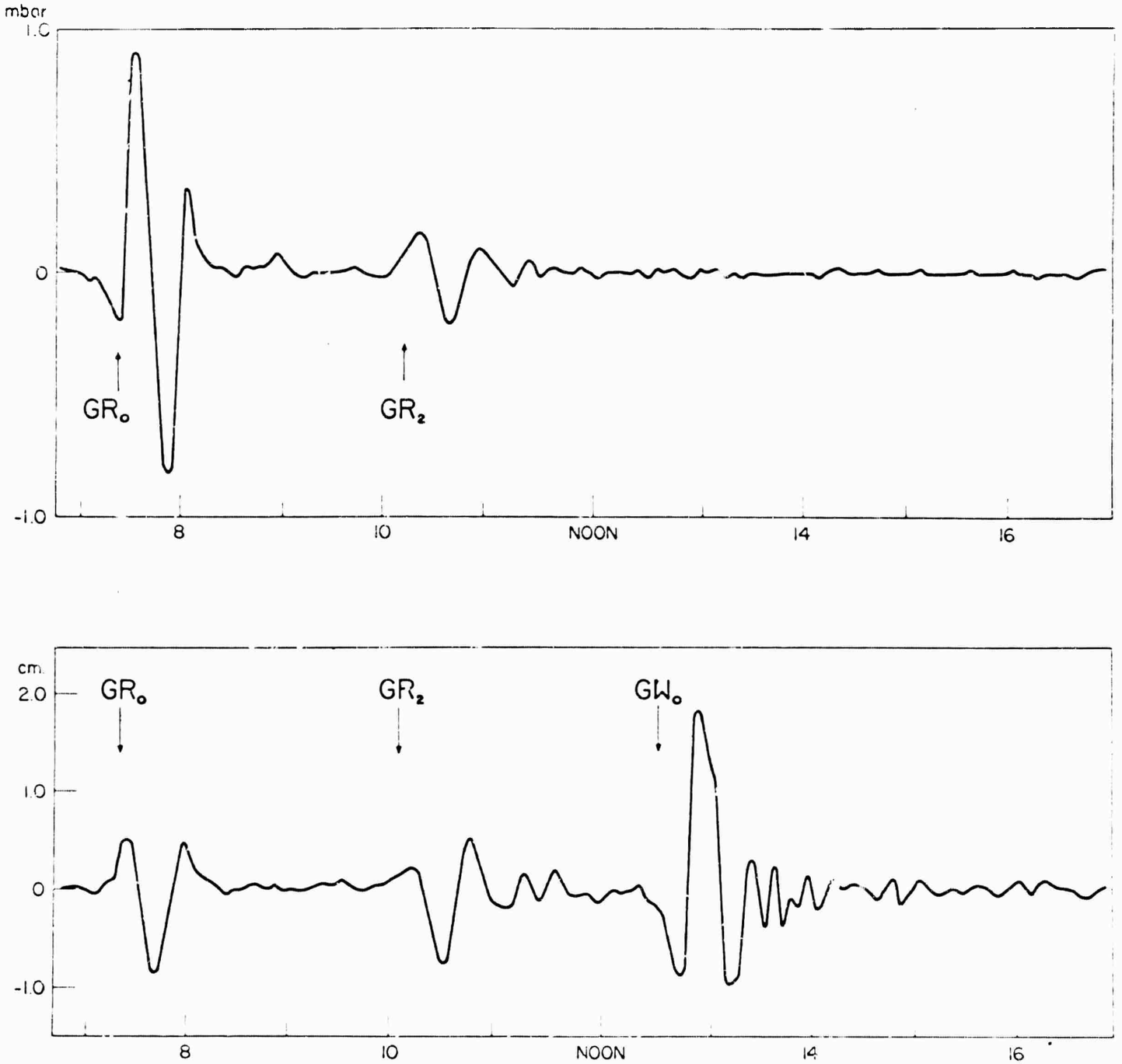
mbar
1.0
0
-1.0
GR₀
GR₂
8
10
NOON
14
16
cm
2.0
1.0
0
-1.0
GR₀
GR₂
GW₀
8
10
NOON
14
16

Fig. 12

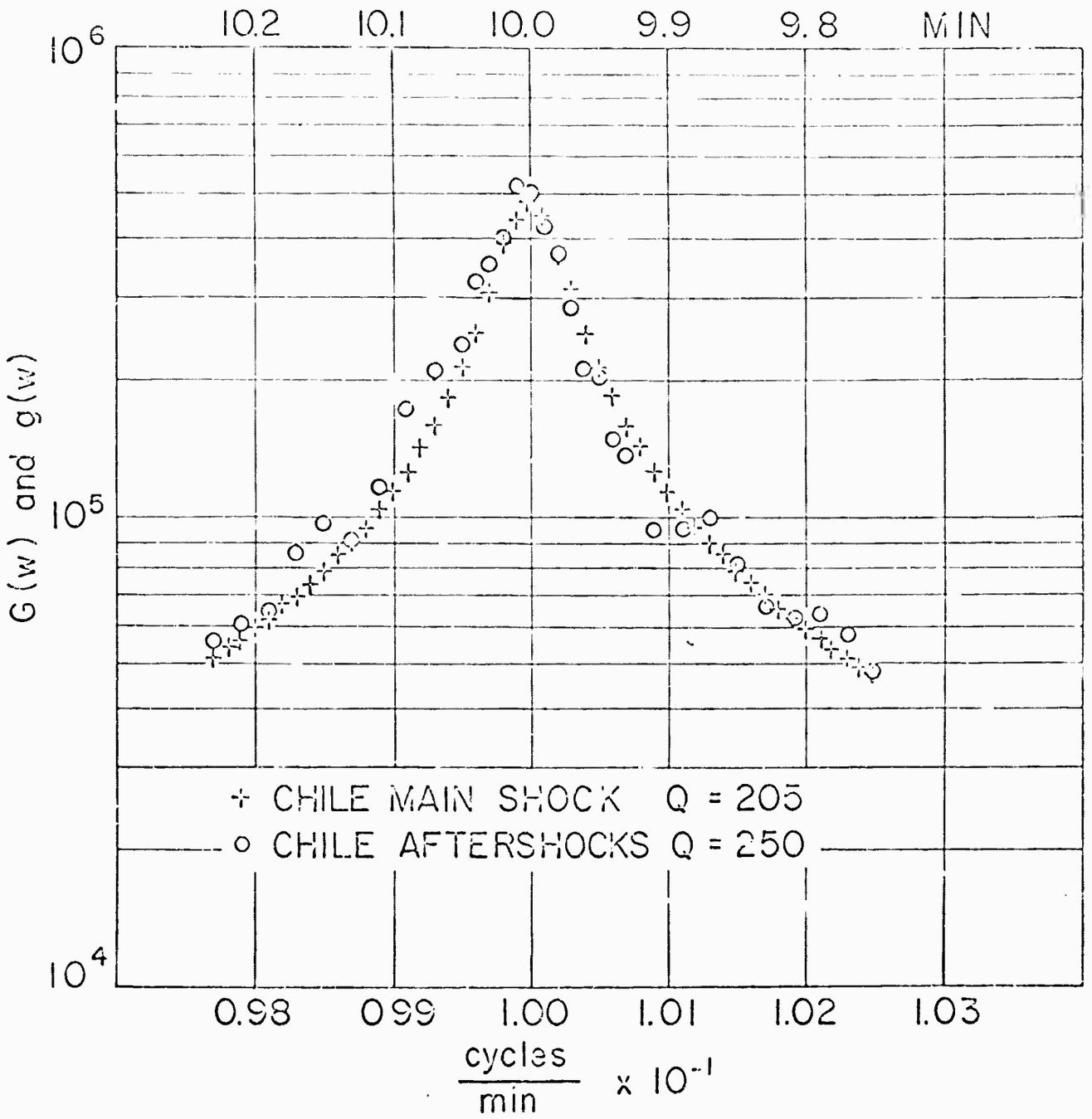
10.2
10.1
10.0
9.9
9.8
MIN
10^6
10^5
10^4
G(w) and g(w)
+ CHILE MAIN SHOCK Q = 205
o CHILE AFTERSHOCKS Q = 250
0.98
0.99
1.00
1.01
1.02
1.03
cycles / min
x 10^{-1}

Fig 13

Fig. 14

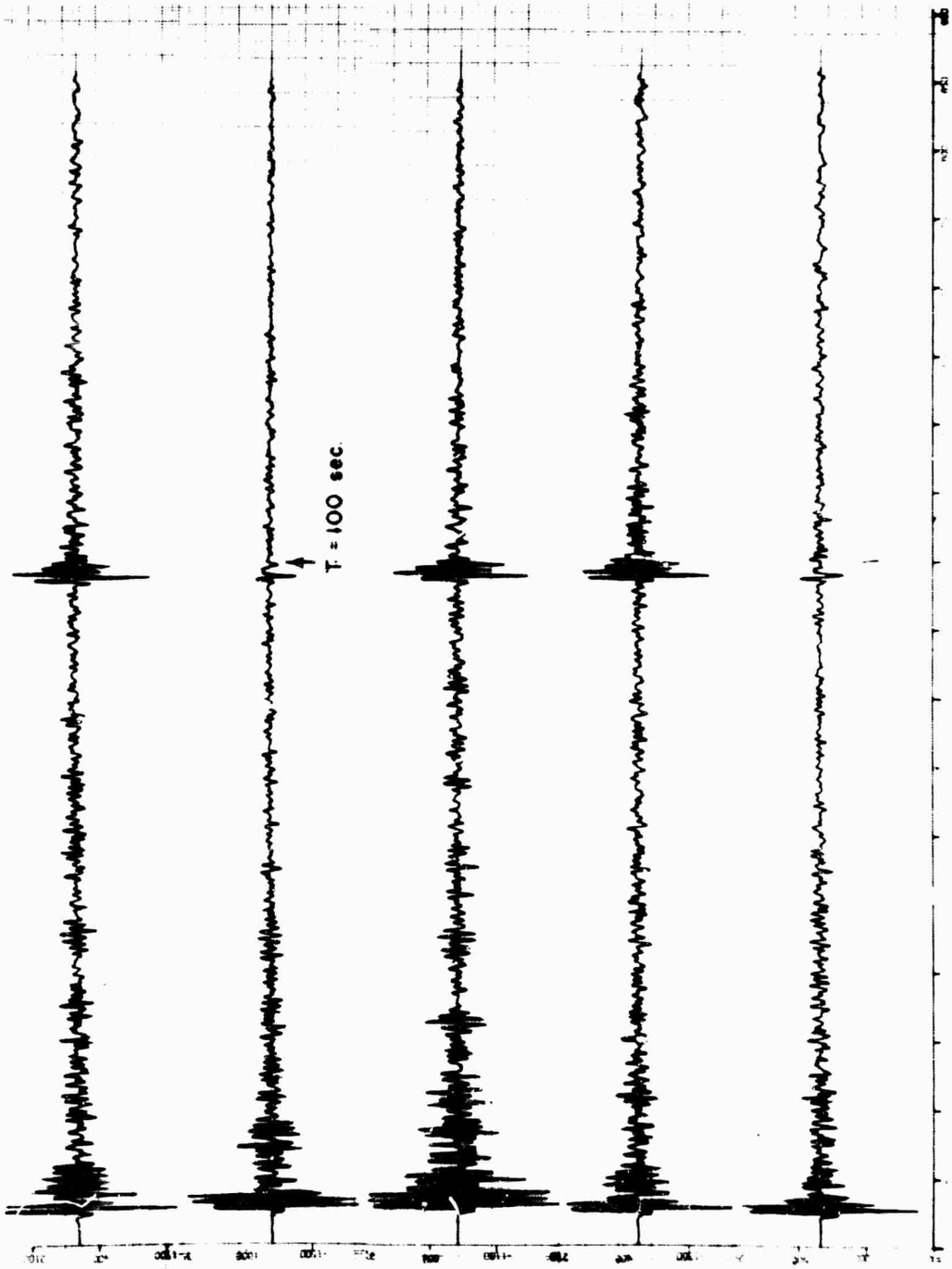

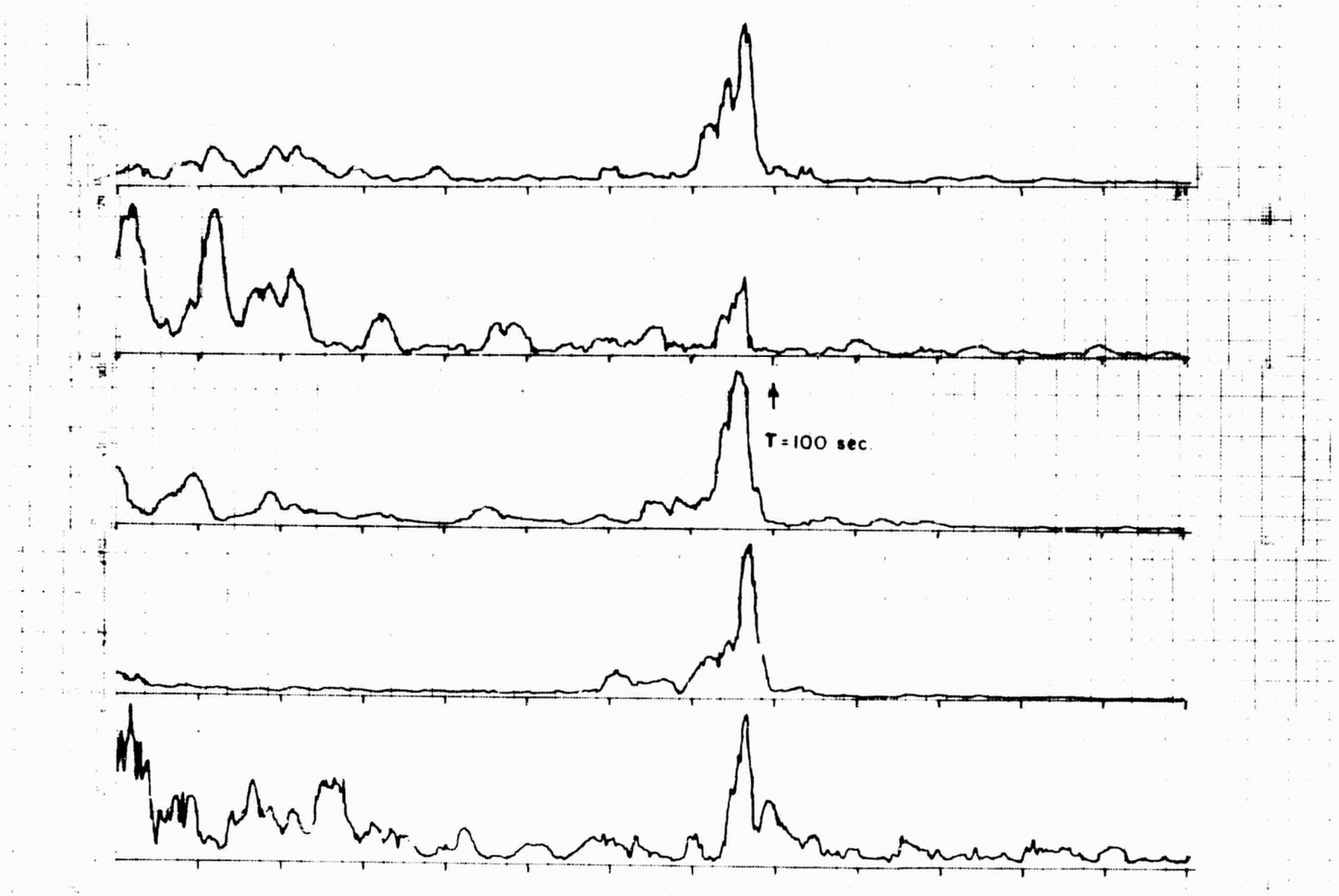

Fig. 15

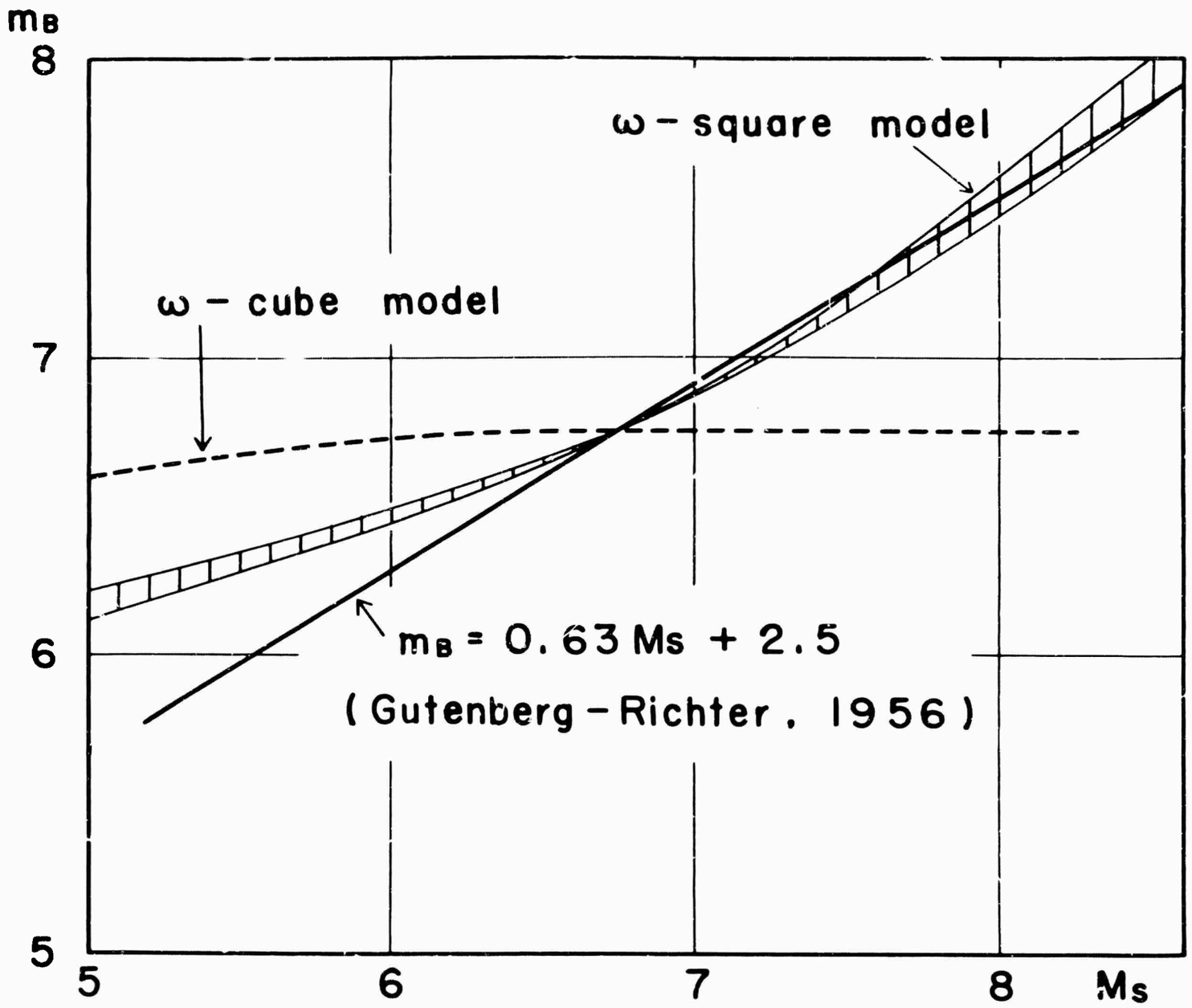
mB
8
7
6
5
5
6
7
8
Ms
ω - square model
ω - cube model
mB = 0.63 Ms + 2.5
(Gutenberg - Richter , 1956)

Fig 9

Fig. 16

Unclassified
Security Classification

DOCUMENT CONTROL DATA - R&D

(Security classification of title, body of abstract and indexing annotation must be entered when the overall report is classified)

1 ORIGINATING ACTIVITY (Corporate author)
Massachusetts Institute of Technology
Department of Geology and Geophysics
Cambridge, Massachusetts 02139

2a REPORT SECURITY CLASSIFICATION
Unclassified

2b GROUP

3 REPORT TITLE

Research in Seismology

4 DESCRIPTIVE NOTES (Type of report and inclusive dates)
Scientific:.....Annual (1 November 1965 - 31 October 1966)

5 AUTHOR(S) (Last name, first name, initial)

Press, Frank and Toksöz, M. Nafi

6 REPORT DATE	7a TOTAL NO. OF PAGES	7b NO. OF REFS
9 December 1966	35	10

8a CONTRACT OR GRANT NO.	9a ORIGINATOR'S REPORT NUMBER(S)
AF 49(638)-1632	M.I.T. Dept. of Geology and Geophysics No: S(Seismology) -2
b PROJECT NO. 8652	
c	9b OTHER REPORT NO(S) (Any other numbers that may be assigned this report)
d	(AFOSR -66-)

10 AVAILABILITY/LIMITATION NOTICES
Distribution of this document is unlimited

11 SUPPLEMENTARY NOTES

12 SPONSORING MILITARY ACTIVITY
Air Force Office of Scientific Research.
(SRPG) 1400 Wilson Blvd.
Arlington, Virginia 22209

13 ABSTRACT

The velocity structure in the earth's mantle is determined using the travel times and travel-time slopes of P-waves recorded at LASA. The results show anomalous velocity gradients at depths of 700, 1200, and 1900 km. Both surface wave dispersion data and $dt/d\Delta$ data show the presence of lateral heterogeneities in the upper and lower mantle.

Theoretical studies of acoustic and gravity wave propagation in the atmosphere-ocean systems, affect of aftershocks on free oscillations, and response of layered spherical earth to point sources have been described.

DD FORM 1 JAN 64 1473

Unclassified
Security Classification

14 KEY WORDS	LINK A		LINK B		LINK C	
	ROLE	WT	ROLE	WT	ROLE	WT
Seismology						
Seismic Velocities						
Earth's mantle						
Gravity waves						
Free Oscillations						
Aftershocks						
Earthquake prediction						
Signal matching						

INSTRUCTIONS

1. ORIGINATING ACTIVITY: Enter the name and address of the contractor, subcontractor, grantee, Department of Defens_ activity or other organization *(corporate author)* issuing the report.

2a. REPORT SECURITY CLASSIFICATION: Enter the overall security classification of the report. Indicate whether "Restricted Data" is included. Marking is to be in accordance with appropriate security regulations.

2b. GROUP: Automatic downgrading is specified in DoD Directive 5200.10 and Armed Forces Industrial Manual. Enter the group number. Also, when applicable, show that optional markings have been used for Group 3 and Group 4 as authorized.

3. REPORT TITLE: Enter the complete report title in all capital letters. Titles in all cases should be unclassified. If a meaningful title cannot be selected without classification, show title classification in all capitals in parenthesis immediately following the title.

4. DESCRIPTIVE NOTES: If appropriate, enter the type of report, e.g., interim, progress, summary, annual, or final. Give the inclusive dates when a specific reporting period is covered.

5. AUTHOR(S): Enter the name(s) of author(s) as shown on or in the report. Enter last name, first name, middle initial. If military, show rank and branch of service. The name of the principal author is an absolute minimum requirement.

6. REPORT DATE: Enter the date of the report as day, month, year; or month, year. If more than one date appears on the report, use date of publication.

7a. TOTAL NUMBER OF PAGES: The total page count should follow normal pagination procedures, i.e., enter the number of pages containing information.

7b. NUMBER OF REFERENCES: Enter the total number of references cited in the report.

8a. CONTRACT OR GRANT NUMBER: If appropriate, enter the applicable number of the contract or grant under which the report was written.

8b, 8c, & 8d. PROJECT NUMBER: Enter the appropriate military department identification, such as project number, subproject number, system numbers, task number, etc.

9a. ORIGINATOR'S REPORT NUMBER(S): Enter the official report number by which the document will be identified and controlled by the originating activity. This number must be unique to this report.

9b. OTHER REPORT NUMBER(S): If the report has been assigned any other report numbers *(either by the originator or by the sponsor)*, also enter this number(s).

10. AVAILABILITY/LIMITATION NOTICES: Enter any limitations on further dissemination of the report, other than those imposed by security classification, using standard statements such as:

(1) "Qualified requesters may obtain copies of this report from DDC."

(2) "Foreign announcement and dissemination of this report by DDC is not authorized."

(3) "U. S. Government agencies may obtain copies of this report directly from DDC. Other qualified DDC users shall request through _____."

(4) "U. S. military agencies may obtain copies of this report directly from DDC. Other qualified users shall request through _____."

(5) "All distribution of this report is controlled. Qualified DDC users shall request through _____."

If the report has been furnished to the Office of Technical Services, Department of Commerce, for sale to the public, indicate this fact and enter the price, if known.

11. SUPPLEMENTARY NOTES: Use for additional explanatory notes.

12. SPONSORING MILITARY ACTIVITY: Enter the name of the departmental project office or laboratory sponsoring *(paying for)* the research and development. Include address.

13. ABSTRACT: Enter an abstract giving a brief and factual summary of the document indicative of the report, even though it may also appear elsewhere in the body of the technical report. If additional space is required, a continuation sheet shall be attached.

It is highly desirable that the abstract of classified reports be unclassified. Each paragraph of the abstract shall end with an indication of the military security classification of the information in the paragraph, represented as *(TS)*, *(S)*, *(C)*, or *(U)*.

There is no limitation on the length of the abstract. However, the suggested length is from 150 to 225 words.

14. KEY WORDS: Key words are technically meaningful terms or short phrases that characterize a report and may be used as index entries for cataloging the report. Key words must be selected so that no security classification is required. Identifiers, such as equipment model designation, trade name, military project code name, geographic location, may be used as key words but will be followed by an indication of technical context. The assignment of links, rules, and weights is optional.